PERFORMANCE ANALYSES OF SUPERCRITICAL ORGANIC RANKINE CYCLES (ORCS) WITH LARGE VARIATIONS OF THE THERMOPHYSICAL PROPERTIES IN THE PSEUDOCRITICAL REGION

TIAN Ran[1], AN Qingsong[2] , SHI Lin[1,*] , ZHAI Huixing[1] and DAI Xiaoye[1]

[1]Key Laboratory for Thermal Science and Power Engineering of Ministry of Education, Department of Thermal Engineering, Tsinghua University,
Beijing, 100084, China
[2]Key Laboratory of Efficient Utilization of Low and Medium Grade Energy, MOE, School of Mechanical Engineering, Tianjin University, Tianjin 300072, China
e-mail: rnxsl@mail.tsinghua.edu.cn and tianr13@mails.tsinghua.edu.cn

ABSTRACT

Transcritical Organic Rankine cycles (ORCs) are more attractive than subcritical ORCs in terms of their lower exergy losses, higher thermal efficiencies and higher work outputs. This study analyzed the influence of the thermophysical properties variations in the pseudocritical region on the transcritical ORCs performance. For various turbine inlet temperatures and vapor generation pressures, the operating parameters were optimized simultaneously considering the net work output, the thermal efficiency and the total vapor generator area. The results show that the total vapor generator area varied with the turbine inlet temperature along an N-shaped curve. For any heat source temperature, the suitable working fluid should have a pronounced N-shaped curve of the total vapor generator area to guarantee the existence of the optimal parameter region in which all three indicators are optimized. This provides a working fluid selection criterion for heat sources of different temperatures. The analysis simplifies the selections of the operating parameters and the working fluids.

1. INTRODUCTION

Organic Rankine Cycles and their many applications for heat recovery from medium and low temperature heat sources have been widely investigated. Much research interest has been focused on transcritical ORCs because of their high thermal efficiencies, exergy efficiencies and work outputs (Schuster e*t al.*, 2010, Karellas and Schuster, 2008, Saleh *et al.*, 2007).

Many studies have considered the working fluid selection and parameter optimization of transcritical ORCs. Maraver *et al.* (2014) provided a general overview of the working fluid selection and optimal design of ORC for different heat sources. They concluded that supercritical cycles are justified for lower critical temperature working fluids if there is no high pressure limitation. However the author did not take into account the working fluid's heat transfer rates. Some researchers have used heat transfer models in heat exchanger area calculations to make economic analyses. Baik *et al.* (2011) compared the transcritical ORC performance of CO_2 and R125 systems using a discretized heat exchanger model to show that R125 has the higher net power output. Li *et al.* (2014) performed thermo-economic analyses with CO2, R123, R600a, R245fa and R601. Zhang *et al.* (2011) compared the performance of subcritical and transcritical power cycles using optimized cycle parameters. R125 in a transcritical power cycle gave excellent economics and maximized the heat source utilization. Guo *et al.* (2014) investigated the

performance of subcritical and transcritical ORCs based on the pinch point locations in the evaporators. Their results showed that transcritical ORCs have better performance when heat source outlet temperatures are lower.

Although much work has been done on optimizing the thermodynamics and economics of ORC cycles, there are few studies of the heat transfer characteristics or the influence of the thermophysical properties. The thermophysical properties in the supercritical pressure region undergo significant changes in the pseudocritical region (Pioro *et al.*, 2011) as shown in Figure 1. These changes affect the working fluid temperature profile and the pinch point location which greatly influence the operating parameter selection and add new requirements to the heat exchanger designs (Karellas *et al.*, 2012). Therefore, the thermophysical properties changes are the key issue for optimization and heat exchanger designs but there are few studies on this topic.

The aims of this study are to investigate the influence of the significant thermophysical property changes in the pseudocritical region on the ORC performance to provide guidance for system designs. First, the turbine inlet temperature, T_3, and the vapor generation pressure, P_{vap}, were optimized using the net work output W_{net} and the thermal efficiency as the indicators. Then, the variations of the vapor generator surface area, A_{total}, that are related to the changes in T_3 and P_{vap} were analyzed based on the thermophysical property changes. An optimal region was discovered by considering all three indicators, W_{net}, the thermal efficiency and A_{total}. A working fluid selection criterion was then developed based on an analysis of the N-shaped curve for A_{total} at various heat source temperatures.

2. SYSTEM MODELING

2.1 System Description

The basic ORC cycle includes a turbine, condenser, pump and vapor generator. As shown in Figure 2, the working fluid is pressurized to supercritical pressures in the pump and heated by the heat source from point 2 to point 3. In the turbine, the working fluid expands to low pressure to produce work. Finally, the lower pressure vapor is condensed to liquid in the condenser. The working fluid R134a was used as an example.

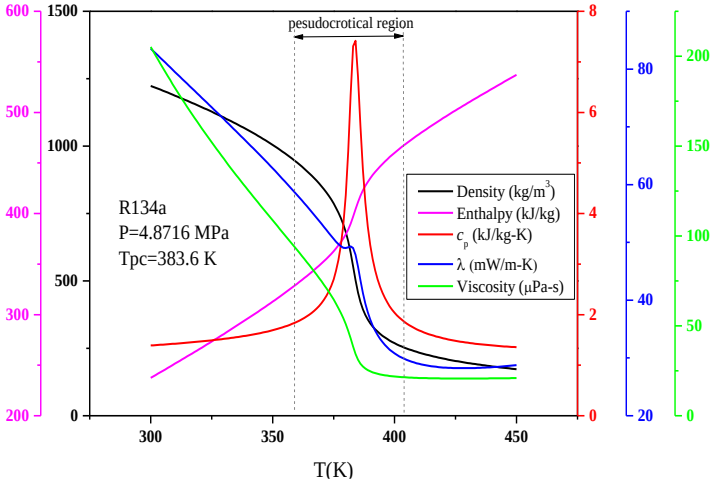

Figure 1: Thermophysical property variations in the pseudocritical region.

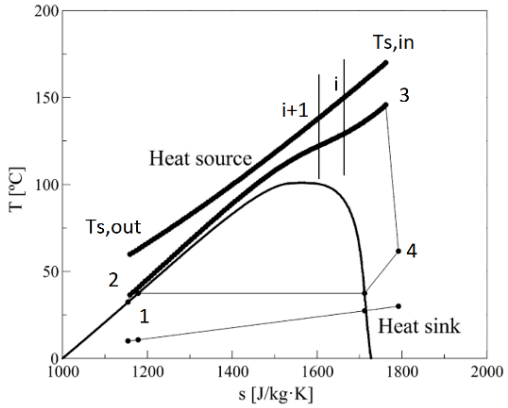

Figure 2: *T-s* diagram for a transcritical ORC system

2.2 Vapor Generator Model

The working fluid is heated in the vapor generator from liquid to vapor without phase change at supercritical pressures. Due to the significant changes in the thermophysical properties, the vapor generator was divided into n sections in a discretized model assuming equal enthalpy differences as shown in Figure 2. The vapor generator was divided into 100 sections, which has been shown to be reasonable in the literature (Karellas *et al.*, 2012). Section 1 was at the heat source inlet and the working fluid outlet with section 100 as the heat source outlet and the working fluid inlet.

The Nusselt number was calculated using the Jackson correlations (Jackson, 2002) for supercritical pressure fluids:

$$Nu = 0.0183\,\mathrm{Re_b}^{0.82}\,\mathrm{Pr_b}^{0.5}\left(\frac{\rho_w}{\rho_b}\right)^{0.3}\left(\frac{\overline{c_p}}{c_{pb}}\right)^{n} \tag{1}$$

Exponent n is:

$n = 0.4$, for $T_b < T_w < T_{pc}$ and for $1.2T_{pc} < T_b < T_w$;

$n = 0.4 + 0.2\left(\frac{T_w}{T_{pc}} - 1\right)$, for $T_b < T_{pc} < T_w$;

$n = 0.4 + 0.2\left(\frac{T_w}{T_{pc}} - 1\right)\left[1 - 5\left(\frac{T_b}{T_{pc}} - 1\right)\right]$, for $T_{pc} < T_b < 1.2T_{pc}$ and $T_b < T_w$

Where b refers to the bulk fluid temperature and w refers to the wall temperature and T_{pc} is the pseudocritical point temperature. The average specific heat of the working fluid was defined as:

$$\overline{c_p} = \frac{h_w - h_b}{T_w - T_b} \tag{2}$$

The convective heat transfer coefficient in the working fluid was:

$$\alpha_{ORC} = \frac{Nu\lambda}{d} \tag{3}$$

The mean overall heat transfer coefficient was:

$$\frac{1}{U} = \frac{1}{\alpha_{\mathrm{ORC}}} + \frac{1}{\alpha_{\mathrm{HS}}} + \frac{\delta}{\lambda} \tag{4}$$

α_{HS} was calculated using the Dittus Boelter correlation (Sharabi *et al.*, 2008):

$$Nu = 0.023 \mathrm{Pr}^{n} \mathrm{Re}^{0.8} \tag{5}$$

Where n=0.4 is for heating processes.

The model assumed no heat losses with the logarithmic mean temperature difference (LMTD) used in each element instead of a global temperature difference:

$$Q_{1-i} = \dot{m}_{\mathrm{ORC}} \cdot \left(h_1 - h_i\right) = \dot{m}_{\mathrm{HS}} \cdot c_{\mathrm{p,HS}} \cdot \left(T_{\mathrm{HS},1} - T_{\mathrm{HS},i}\right) \tag{6}$$

The total vapor generator area, A_{total}, was:

$$A_{\mathrm{total}} = \sum_{i=1}^{i=n} A_i \tag{7}$$

2.3 Global Model

There is no isothermal boiling in the transcritical ORC, so the pinch point location cannot be determined as easily as for the subcritical ORC. The temperature profiles in both the heat source fluid and the working fluid in the vapor generator were calculated using the vapor generator model for the model parameters listed in Table 1. The pinch point location was then determined by modifying the working fluid mass flow rate to get the designed pinch point temperature difference.

Table 1: Simulation parameters for ORC model

Part	Items	Values
Heat source	Inlet temperatures (°C)	160, 170, 180, 190
	Mass flow rate (kg/s)	1
	Pipe pressure (MPa)	1.3
ORC cycle	Pinch point temperature difference (°C)	10
	Condensing temperature (°C)	30
	Isentropic pump efficiency	0.65
	Isentropic turbine efficiency	0.85

3. RESULTS AND DISCUSSION

The calculation used R134a as the working fluid and a 170°C heat source for the parameter optimization (section 3.1) and vapor generator area analysis (section 3.2). R152a and R245fa were used for higher heat source temperatures in section 3.3.

3.1 Parameter optimization based on W_{net} and the thermal efficiency

W_{net} and the thermal efficiency were optimized by changing the turbine inlet temperature, T_3, and the vapor generation pressure P_{vap}. As shown in Figure 3(a), an optimal W_{net} exists at each P_{vap}. Further, the peak W_{net} move towards higher T_3 as P_{vap} increases. The maximum W_{net} was reached at $1.6P_{\mathrm{c}}$ with only small differences in the maximum W_{net} for various P_{vap}. For example, the maximum W_{net} at 1.3 P_{c} is only 1.14% smaller than that at 1.6 P_{c}. Therefore, lower vapor generation pressures should be used to reduce the component requirements and the initial cost with little difference in the work output.

As shown in Figure 3(b), the thermal efficiency increases with T_3 as has been seen in many studies. The thermal efficiency variations with P_{vap} depend on the turbine outlet conditions. For lower T_3 ($T_3 <$ 393.15K), the thermal efficiency decreases with P_{vap} while higher T_3 ($T_3 >$ 393.15K) have maximum thermal efficiency as P_{vap} varies.

Figure 4 shows the variations of W_{net} and the thermal efficiency in response to T_3 and P_{vap}. The shaded area in Figure 4(c) is the optimal region for both W_{net} and the thermal efficiency.

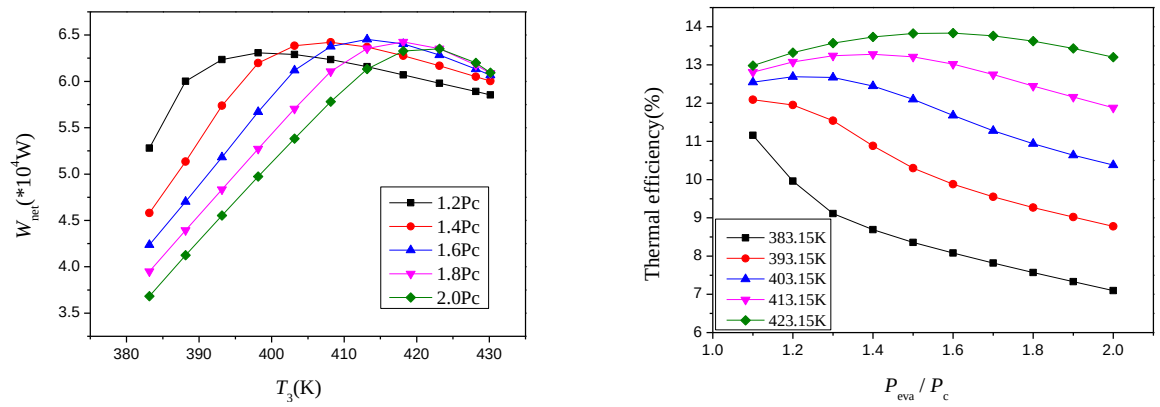

(a) (b)

Figure 3: (a) Net work outputs for various turbine inlet temperatures and vapor generator pressures and (b) thermal efficiencies for various vapor generator pressures and turbine inlet temperatures (R134a, T_s=170ºC)

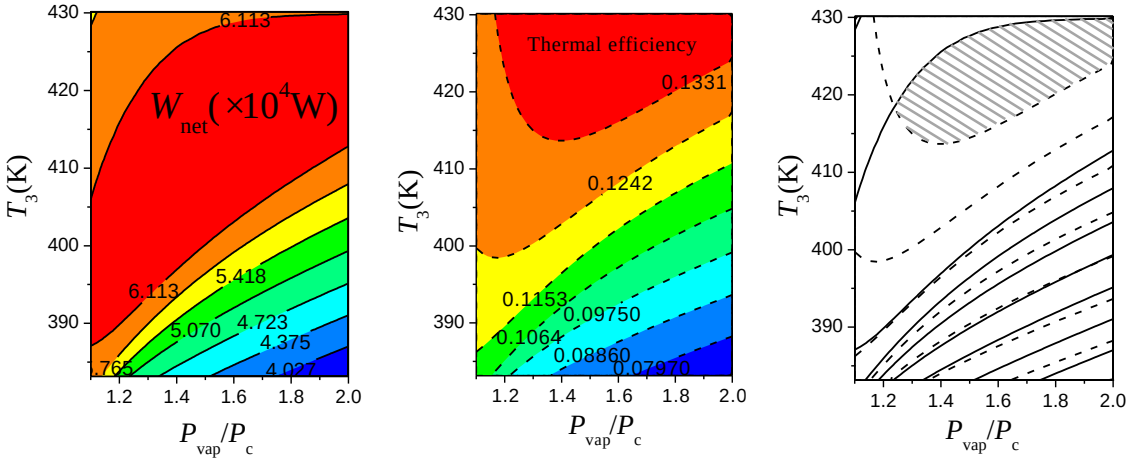

(a) (b) (c)

Figure 4: (a) W_{net} for various T_3 and P_{vap}, (b) thermal efficiency for various T_3 and P_{vap} and (c) the optimal operating conditions.

3.2 Vapor Generator Area Analysis

The vapor generator heat exchanger area is the third optimization indicator. The special characteristics of heat transfer at supercritical pressures need to be illustrated by showing the influence of the ORC parameters on the heat exchanger area. Figure 5 shows that the total vapor generator area varies with the turbine inlet temperature along an N-shaped curve.

The N-shaped curve is caused by the variations of the heat transfer coefficient and the LMTD in the pseudocritical region and the movement of the pinch point location. The heat transfer is strongly

affected by the significant changes in the thermophysical properties. As shown in Figure 6(a), the convection heat transfer coefficient of R134a has a peak at temperatures slightly lower than the pesudocritical point and then decreases sharply. The enthapy sharply increases in the pseudocritical region as shown in Figure 1, so the working fluid temperature gradient, dT/dn, is almost equal to zero, resulting in the temperature profile shown in Figure 6(b). This temperature profile means that the pinch point cannot move across the pseudocritical region. With increasing T_3, the pinch point moves from the heat source outlet towards the middle, staying at the lower temperature side of the pseudocritical region in the end as shown in Figure 7. The variation of LMTD shown in Figure 8(a) coincides with the temperature profile shown in Figure 6(b), which is the result of the enthalpy variation in the pseudocritical region. In each section of the vapor generator, the elementary area A_i is inversely proportional to the heat transfer coefficient and LMTD, so A_i varies as shown in Figure 8(b). A_{total} is the sum of A_i. Thus, the variations of the heat transfer coefficient and the LMTD in the pseudocritical region and the movement of the pinch point location result in the N-shaped curve for A_{total}.

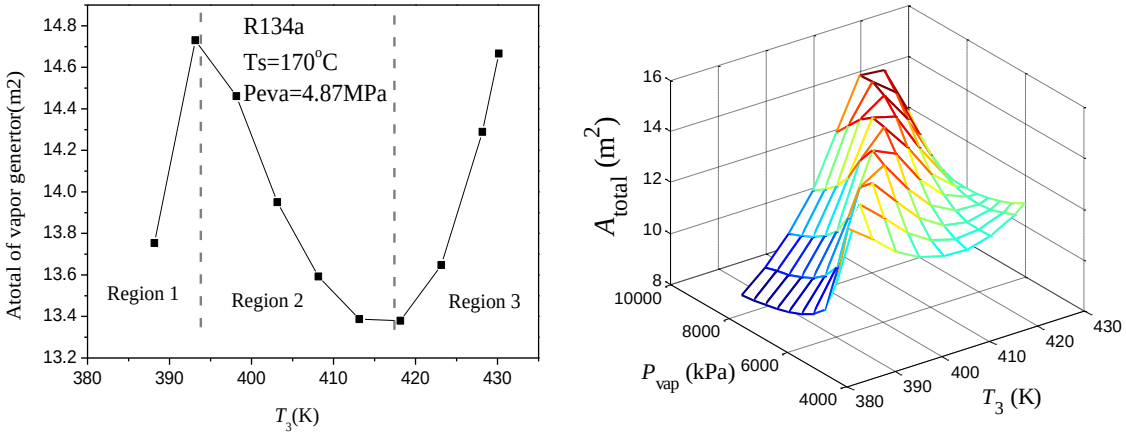

(a) (b)

Figure 5: (a) Variation of the vapor generator area A_{total} with the turbine inlet temperature and (b) the variation of A_{total} with the vapor generation pressure and turbine inlet temperature.

A_{total} can be used as the third optimization indicator along with W_{net} and the thermal efficiency. The N-shaped curve in Figure 5(a) can be divided into three regions:

Region 1: T_3=388.15-393.15 K. The pinch point moves from the heat source outlet to the inlet with increasing T_3 as shown in Fig. 8. A_{total} increases with T_3 with the minimum at 388.15 K. However, the transcritical ORC has low W_{net} and thermal efficiency in this region. Therefore, the system should not operate in this region.

Region 2: T_3=393.15-418.15 K. The pinch point moves to the heat source inlet and A_{total} begins to decrease with T_3. In this region, both W_{net} and thermal efficiency are relatively high, so the system should operate in this region.

Region 3: T_3>418.15 K， A_{total} increases rapidly in this region due to the higher T_3 and the heat transfer coefficient in this region being much lower than in the other two regions so the heat exchanger area is wasted . For economic reasons, the system should not operate in this region.

The influence of pressure on A_{total} is shown in Figure 5(b). A higher vapor generation pressure results in a larger heat exchanger. Therefore, higher pressures are not economical. The final optimization results considering all three indicators, W_{net}, η_{th} and A_{total}, are shown in Figure 9(b) as the shaded area.

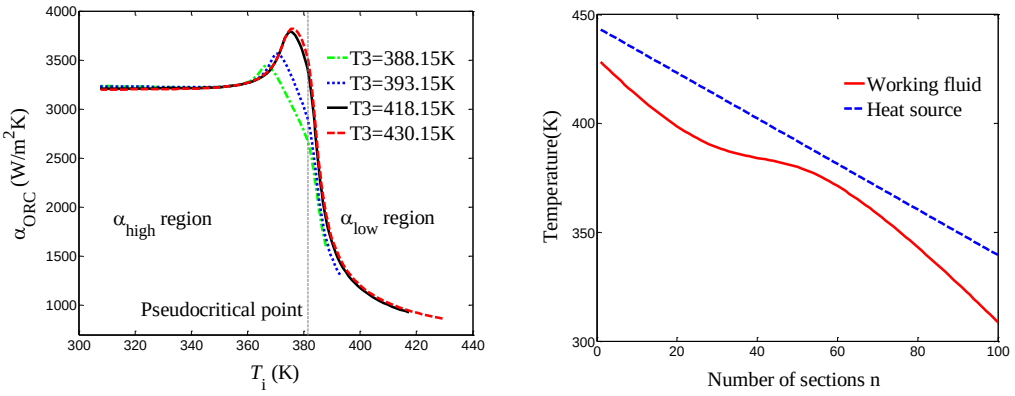

(a) (b)

Figure 6: (a) Convection heat transfer coefficient of working fluid in the vapor generator for various turbine inlet temperatures and (b) working fluid and heat source temperature profiles in the vapor generator.

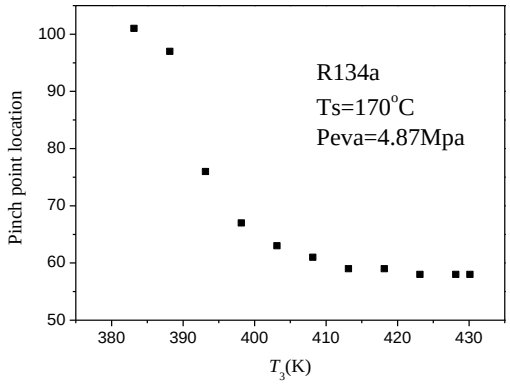

Figure 7: Pinch point locations for various turbine inlet temperatures

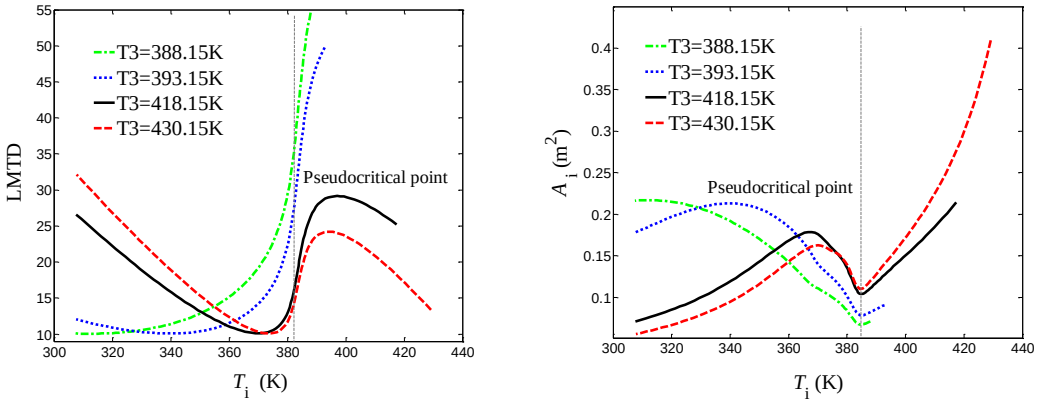

(a) (b)

Figure 8: (a) LMTD variations in the vapor generator for various turbine inlet temperatures and (b) the elementary surface area A_i variations in the vapor generator for various turbine inlet temperatures.

3.3 Working Fluid Selection Criterion at Various Heat Source Temperatures

The system performance was also investigated for various heat source temperatures. R134a was used in sections 3.1 and 3.2 with a 170°C heat source. Other heat source temperatures will require other working fluids so that the system has an optimal region as in Figure 9(b). As shown in Table 2, when

the heat source temperature increases from 160°C to 190°C, the higher temperature heat source gives a larger maximum W_{net}, but the corresponding optimal pressure increases from 6.09 MPa to 7.71 MPa. The higher pressure make the system more dangerous and difficult to maintain. As shown in Figure 10, the N-shaped curve of A_{total} for R134a is less pronounced with A_{total} in region 2 increasing significantly with the increasing heat source temperature. Moreover, the higher heat source temperature keeps the pinch point at the heat source outlet as shown in Figure 11. Since the system performance is worse when the pinch point is adjacent to the heat source outlet, the higher heat source temperature will lead to poor performance and there is no optimal shaded area as in Figure 9(b).

In conclusion, when the heat source temperature is much higher than T_c of the working fluid, the optimal area does not exist. While R134a performs well with a 170°C heat source, R134a is not suitable for higher temperature heat sources of 180-190°C. The results in Table 2 show that $W_{net,max}$ and the thermal efficiency of R152a, R245fa, whose T_c are higher than that of R134a, are both higher than that of R134a. The optimal pressures are also much lower than that of R134a for the same heat source temperature. Figures 10 and 11 show that the A_{total} in region 2 using R152a and R245fa are much lower than that of R134a and the pinch point quickly moves to the lower temperature side of the pseudocritical region. The performance is greatly improved by using R152a and R245fa with the 190°C heat source. Thus, if the N-shaped curve for A_{total} is less pronounced or disappears and the pinch point is always stay near heat source outlet, then the current working fluid cannot match the heat source and working fluids with higher critical temperatures are suggested.

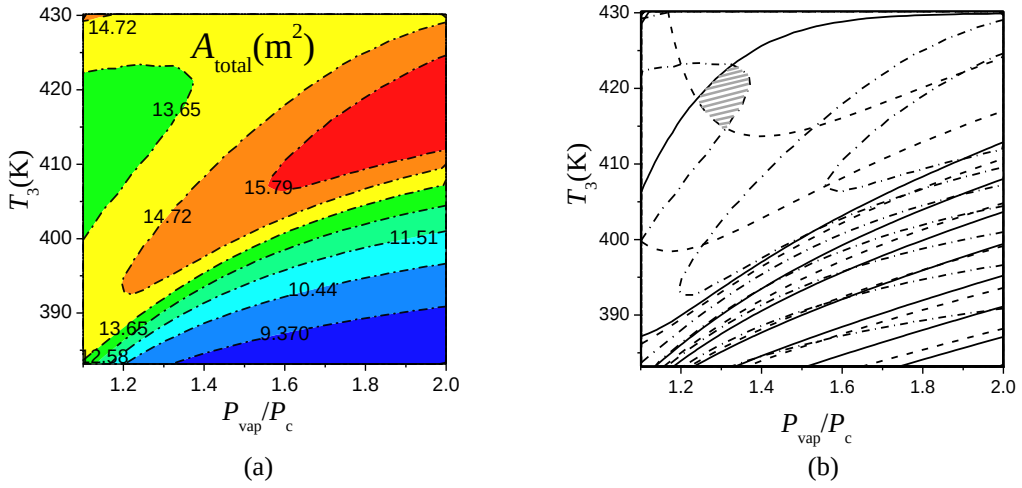

Figure 9: (a) A_{total} variations with T_3 and P_{vap} and (b) the optimal operating region

Table 2: Optimal operating parameters with W_{net} as the optimization objective

	T_c (°C)	P_c (MPa)	T_s (°C)	$W_{net,max}$ (kW)	P_{vap} (MPa)	η_{th} (%)
R134a	101.06	4.0593	160	55.4	6.089	12.10
			170	64.5	6.495	13.02
			180	73.9	6.901	13.76
			190	83.4	7.713	14.29
R152a	113.26	4.5168	180	73.5	6.324	13.85
			190	83.6	6.775	14.70
R245fa	154.01	3.651	190	90.4	4.746	15.22

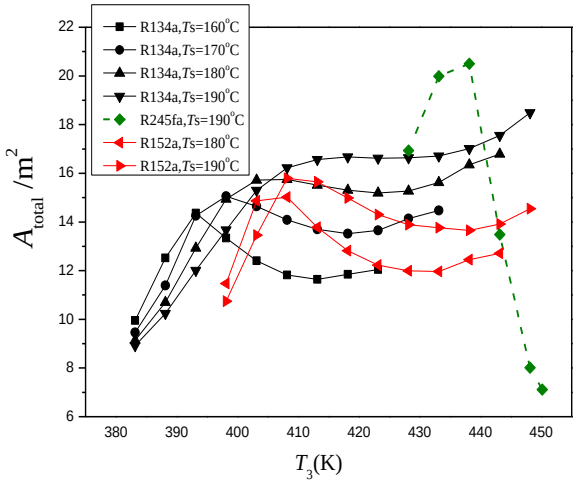

Figure 10: A_{total} variations with the turbine inlet temperature for various heat source temperatures

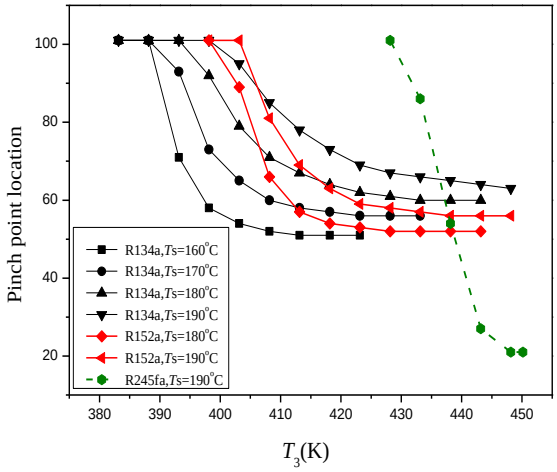

Figure 11: Pinch point location variations with the turbine inlet temperature

4. CONCLUSION

The influence of the large changes in the thermophysical properties in the pseudocritical region was investigated. An optimization method was developed using the net work output, the thermal efficiency and the total vapor generator area. The optimal turbine inlet temperature and vapor generation pressure were found for various operating conditions. The results obtained in this study will simplify working fluid selection for various heat source temperatures. The main conclusions can be summarized as:

1. The thermophysical properties of the working fluid in transcritical ORCs operating at supercritical pressure undergo significant changes, resulting in considerable variations in the heat transfer coefficient and LMTD. Therefore, studies of transcritical ORCs should pay much more attention to the thermophysical property changes in the pseudocritical region. The heat transfer mechanisms at supercritical pressure must be further understood for system optimization and proper heat exchanger design.
2. The total vapor generator area, A_{total}, varies with the turbine inlet temperature T_3 along an N-shaped curve due to the variations of heat transfer coefficient and LMTD in the pesudocirtical region and the changes of the pinch point location. The optimal operating conditions should be in region 2 of

the N-shaped curve to give the best area with the best W_{net} and thermal efficiency.

3. A working fluid selection criterion was developed for various heat source temperatures. A suitable working fluid should have a pronounced N-shaped curve for A_{total} to guarantee the existence of the optimal parameter region. When the N-shaped curve for A_{total} is less pronounced or non-existent and the pinch point is always near the heat source outlet, the working fluid cannot match the heat sources, and working fluids with higher critical temperatures are suggested.

REFERENCES

Baik, Y. J., Kim, M., Chang, K. C., & Kim, S. J. (2011). Power-based performance comparison between carbon dioxide and R125 transcritical cycles for a low-grade heat source. *Applied Energy*, *88*(3), 892-898.

Guo, C., Du, X., Yang, L., & Yang, Y. (2014). Performance analysis of organic Rankine cycle based on location of heat transfer pinch point in evaporator. *Applied Thermal Engineering*, *62*(1), 176-186.

Jackson JD. Consideration of the heat transfer properties of supercritical pressure water in connection with the cooling of advanced nuclear reactors, Proc. 13th Pacific Basin Nuclear Conference, Shenzhen City, China, October 21 – 25, 2002

Karellas, S., & Schuster, A. (2008). Supercritical fluid parameters in organic Rankine cycle applications. *International Journal of Thermodynamics*, *11*(3), 101-108.

Karellas, S., Schuster, A., &Leontaritis, A. D. (2012). Influence of supercritical ORC parameters on plate heat exchanger design. *Applied Thermal Engineering*, *33*, 70-76.

Li, M., Wang, J., Li, S., Wang, X., He, W., & Dai, Y. (2014). Thermo-economic analysis and comparison of a CO 2 transcritical power cycle and an organic Rankine cycle. *Geothermics*, *50*, 101-111.

Maraver, D., Royo, J., Lemort, V., &Quoilin, S. (2014). Systematic optimization of subcritical and transcritical organic Rankine cycles (ORCs) constrained by technical parameters in multiple applications. *Applied energy*,*117*, 11-29.

Pioro, I., Mokry, S., & Draper, S. (2011). Specifics of thermophysical properties and forced-convective heat transfer at critical and supercritical pressures. *Reviews in Chemical Engineering*, *27*(3-4), 191-214.

Saleh, B., Koglbauer, G., Wendland, M., & Fischer, J. (2007). Working fluids for low-temperature organic Rankine cycles. *Energy*, *32*(7), 1210-1221.

Schuster A, Karellas S, Aumann R. (2010) Efficiency optimization potential in supercritical Organic Rankine Cycles[J]. Energy, 35(2): 1033-1039.

Sharabi M., W. Ambrosini, S. He, J.D. Jackson, (2008) Prediction of turbulent convective heat transfer to a fluid at supercritical pressure in square and triangular channels, Annals of Nuclear Energy 35 993e1005

Zhang, SJ, Wang, HX, & Tao, G. (2011). Performance comparison and parametric optimization of subcritical Organic Rankine Cycle (ORC) and transcritical power cycle system for low-temperature geothermal power generation. *Applied Energy*, *88*(8), 2740-2754.

ACKNOWLEGEMENTS

This work was supported by the State Key Program of the National Natural Science Foundation of China (Grant No.51236004) and the Science Fund for Creative Research Groups (No. 51321002)